Paucity of chromatic linear motion detectors in macaque V1

Gregory D. Horwitz

Vision Center Laboratory, The Salk Institute for Biological Studies, La Jolla, CA, USA

Thomas D. Albright

Vision Center Laboratory, The Salk Institute for Biological Studies, La Jolla, CA, USA

The motion of a color-defined edge is often more difficult to perceive than the motion of a luminance-defined edge. Neurons subserving motion vision may therefore be particularly sensitive to luminance contrast. One class of neurons thought to play a critical role in motion perception is V1 neurons whose spatiotemporal receptive fields are oriented in space-time. We used the reverse correlation technique to study the relationship between color tuning and space-time receptive field orientation in V1 neurons of awake, fixating monkeys. Neurons with space-time oriented receptive fields were tuned almost exclusively for luminance, whereas neurons with nonoriented space-time receptive fields were tuned for luminance or for color. These results suggest that the special role of luminance contrast in motion perception is due in part to the establishment of space-time oriented receptive fields among luminance-tuned, but not color-tuned, V1 neurons.

Keywords: color, motion, V1, macaque, space-time receptive field orientation

Introduction

The front end of the "first-order motion system" can be modeled as a bank of space-time oriented filters that, in combination with an output nonlinearity, provide a greater output for one direction of motion than the opposite direction (Adelson & Bergen, 1985; Watson & Ahumada, 1985). Some V1 neurons have space-time oriented receptive fields (RFs) and respond approximately like linear filters whose output is put through a threshold nonlinearity (McLean & Palmer, 1989; Reid, Soodak, & Shapley, 1987; but see Emerson, 1997), suggesting that they may be the front end of the first-order motion system. The first-order motion system is specialized for processing luminant over chromatic motion (Cavanagh & Mather, 1989). If V1 neurons with space-time oriented RFs are the front end of the first-order motion system, we might expect these neurons to be tuned preferentially for luminance. The experiments reported here tested this hypothesis.

Direction selectivity, a neuronal property related to space-time RF orientation, has been shown to be correlated with luminance-tuning in many studies (Gouras, 1974; Hubel & Livingstone, 1990; Livingstone & Hubel, 1984; Tamura, Sato, Katsuyama, Hata, & Tsumoto, 1996). Other studies have looked for, and failed to find, such a relationship (Leventhal, Thompson, Liu, Zhou, & Ault, 1995; Michael, 1978a, 1978b). Interpreting the results of these studies is complicated by the facts that they used only limited sets of colored stimuli and did not measure color tuning and direction selectivity with identical stimuli.

Conway, Hubel, and Livingstone (2002) found that L/M cone-opponent V1 cells lack space-time oriented RFs. In a later study, this group showed that some V1 neurons did have space-time oriented RFs when tested with achromatic stimuli (Conway & Livingstone, 2003; Livingstone & Conway, 2003). These results are consistent with the idea that space-time RF orientation is correlated with luminance tuning, but leaves open the possibility that some space-time oriented cells may be tuned primarily for color but responsive to achromatic stimuli.

The goal of the current experiments was to measure space-time RF orientation and color tuning simultaneously and to quantify their relationship rigorously. We stimulated V1 neurons in awake, fixating monkeys with a randomly modulated colorful stimulus. Reverse correlation of the stimulus sequence with recorded spike trains revealed the linear RF maps of these cells and thereby provided estimates of their chromatic and spatiotemporal filtering properties. Based on this analysis, we classified neurons into "luminance" and "color" categories and quantified their space-time RF orientation. Some neurons in each category had nonoriented space-time RFs. In contrast, almost all strongly space-time oriented RFs were observed in luminance-tuned cells. We thus conclude that space-time orientation tuning is an almost exclusive property of luminance-tuned cells. This result strengthens the idea that luminance-tuned direction-selective simple cells in area V1 are key components of the first-order motion system.

Methods

The visual stimulus shown in Figure 1 has been described previously (Horwitz, Chichilnisky, & Albright, 2005). Briefly, the stimulus was an 8 x 8 checkerboard subtending 1.8° of visual angle on a CRT screen (Sony F500). Every video refresh (every 10 ms), the color of each square in the checkerboard changed randomly. Colors were determined by independent draws from red, green, and blue Gaussian phosphor intensity distributions. The mean values of these distributions were the same as the phosphor

doi:10.1167/5.6.4 Received November 5, 2004; published June 17, 2005 ISSN 1534-7362

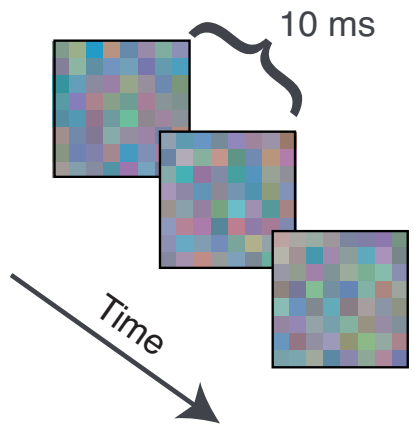

Figure 1. The visual stimulus. The color of each 0.22 x 0.22° pixel in the stimulus was determined by independent draws from Gaussian intensity distributions on the red, green, and blue monitor phosphors.

contributions to the background, which was metameric with an equal energy white at 65 cd/m^2. The standard deviations of these distributions were typically 9% of the range physically achievable, corresponding to luminance contrasts of 3.9, 11.5, and 2.5% for the red, green, and blue phosphors, respectively.

Monkeys were rewarded on a random schedule for fixating a 0.2° x 0.2° black square in the center of the screen while the stimulus was presented at the RF of one or more individually recorded neurons. Fixation breaks suspended reward delivery and extinguished the stimulus.

Extracellular action potentials were recorded with parylene-coated platinum-iridium electrodes (Fredrick Haer) and identified by time, amplitude, and template-matching criteria either online (Alpha Omega) or offline (Plexon). To calculate a spike-triggered average stimulus (STA), spike trains were represented as the number of spikes recorded during each stimulus frame and cross-correlated with the stimulus sequence. Under a linear-nonlinear cascade model, the STA provides an unbiased estimate of the underlying linear filter (Chichilnisky, 2001).

To study the temporal envelope of the response, we cross-correlated the stimulus with the spike train at every lag from 0 ms to 200 ms in 10-ms steps. At a 0-ms lag, the STA was completely unstructured because this lag is shorter than the response latency of the cell. At longer lags (around 40 to 70 ms), the STA contained structure that revealed the average stimulus to which the cell responded. At still longer lags, the structure disappeared as the lag exceeded the cell's "memory." We used a maximum lag of 200 ms because none of the cells we studied had STAs that were structured beyond this lag.

Each STA consisted of 3840 numbers (20 frames x 8 pixels x 8 pixels x 3 phosphors) and can be represented as the space-time volume in Figure 2A. Alternatively, the STA can be represented as a 1280 x 3 matrix, as shown in Figure 2B, in which each row is the average red, green, and blue phosphor intensities for a particular space-time pixel in the STA. Phosphor intensities were expressed relative to the background level: Positive numbers represented intensity increments and negative numbers represented intensity decrements.

To collapse this collection of phosphor intensity triplets into a single triplet that characterized the STA as well as possible, we used a singular value decomposition (SVD) (Strang, 1988). This procedure assumes that the RF is separable in color and space-time, which was approximately true for most of the neurons we studied. The results of the SVD, shown in Figure 2C, are a spatiotemporal weighting function (a 1280 x 1 vector) and a color weighting function

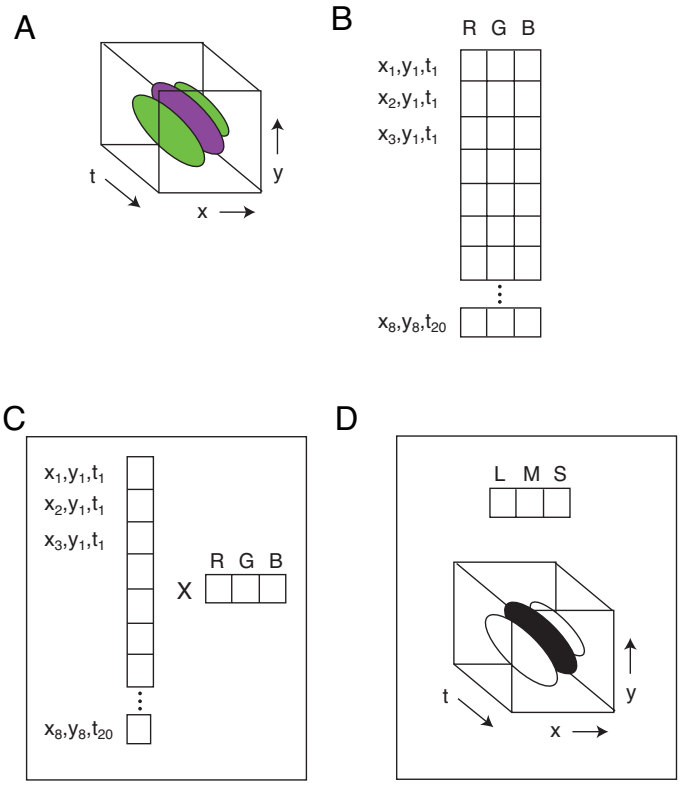

Figure 2. Derivation of cone weights and spatiotemporal weighting function. The spike-triggered average stimulus (STA) is defined as the average space-time-color stimulus that preceded a spike (see Methods) and can be represented as a space-time volume of colored pixels (A). To separate the color weighting function from the spatiotemporal weighting function, we represented the STA as a 1280 x 3 matrix (B) and decomposed this matrix by singular value decomposition. The first column and row eigenvectors of this decomposition were defined as the spatiotemporal weighting function and the color weighting function, respectively (C). The spatiotemporal weighting function (D, bottom) can be represented as a space-time volume of grayscale pixels, because the additional dimension of color has been removed. We transform the color weighting function obtained from the singular value decomposition to cone weights (D, top) by a matrix multiplication.

(a 1 x 3 vector). Other components of the decomposition were discarded.

We transformed the color weighting function to cone weights by the following formula:

$$[lms] = \mathbf{A}^{-T}[rgb]^{T} \quad , \tag{1}$$

where **A** is a 3 x 3 matrix composed of the pairwise dot products of the three cone fundamentals (Stockman, MacLeod, & Johnson, 1993) and the three phosphor emission spectra measured for our monitor. This matrix is inverted and transposed to reflect the fact that the STA represents a visual mechanism that exists in the dual space of lights (Knoblauch & D'Zmura, 2001).

A change in sign of the color weighting function can be compensated for exactly by a change in sign of the spatiotemporal weighting function (Figure 2C). Thus, the overall sign of the cone weight vector is not meaningful without specification of the sign of the spatiotemporal weighting function. We therefore arbitrarily assign all M cone weights to be positive, following the convention of Johnson, Hawken, and Shapley (2004).

Space-time orientation analysis

To quantify space-time orientation, we first reshaped the 1280 x 1 spatiotemporal weighting function to a volume with dimensions 20 frames x 8 pixels x 8 pixels, shown in Figure 2D. We then subjected space-time slices from this volume to two-dimensional (2D) Fourier transformation. We defined a space-time orientation index (STOI) as

$$STOI = \left|(p_1 + p_3) - (p_2 + p_4)\right| \quad , \tag{2}$$

where p_i represents the proportion of the total power in the i^{th} quadrant of the Fourier plane. A RF that is unoriented in space-time will have an STOI close to 0, and a RF that is strongly oriented will have an STOI close to 1.

For each neuron, we calculated STOIs from a horizontal and a vertical slice through the spatiotemporal weighting function passing through the RF center. The larger of these two STOIs was taken as the STOI of the neuron. Our central result, that space-time orientation is more common among luminance-tuned than color-tuned cells, was unchanged when we considered additional slices along the 45° obliques, or when we calculated the root mean square of the STOIs instead of selecting the maximal one.

The STOI depends on the noise in the spatiotemporal weighting function. Intuitively, a perfectly noiseless, strongly oriented spatiotemporal weighting function will have an index of 1 and noise will reduce this value by adding power at spatiotemporal frequencies to which the cell is insensitive. To permit a fair comparison of the value of the STOI across cells, we measured the signal-to-noise ratio of each spatiotemporal weighting function. We express the signal-to-noise ratio as the standard deviation of the elements in the spatiotemporal weighting function divided by the standard deviation of the elements in a spatiotemporal weighting function calculated at a noncausal latency (starting at the time of a spike and extending 200 ms into the future).

Space-space orientation analysis

To determine whether color and luminance cells differ with respect to their spatial orientation tuning, we calculated for each cell a space-space orientation tuning index (SSOI), which is conceptually similar to the STOI just described. To calculate the SSOI, we extracted the unique slice through the peak of the spatiotemporal weighting function that was orthogonal to the two slices considered in the calculation of the STOI.

Oblique orientation in space-time is consistent with direction selectivity, but horizontal and vertical orientations are not. The STOI is therefore constructed so that it equals 0 for horizontally or vertically oriented spatiotemporal weighting functions. In space, on the other hand, oblique orientation has no such privileged status. To quantify spatial orientation tuning, we subjected the extracted spatial weighting function to a 2D Fourier transform and found the spatial frequency pair (ω_x, ω_y) at which the power was greatest (excluding the DC component). We then compared this power (p_a) to the power at the complementary pair of spatial frequencies ($-\omega_y$, ω_x) (p_b), by the following formula:

$$SSOI = \frac{(p_a - p_b)}{p_a} \quad . \tag{3}$$

For a linear neuron, this procedure is equivalent to comparing responses to the optimal spatial frequency sinewave grating at the preferred orientation and at the orthogonal orientation. This index is 0 for a cell that is not tuned for orientation and 1 for a cell that is strongly tuned for orientation.

Results

We recorded from 190 V1 neurons from four monkeys. RFs ranged in eccentricity from 1.6 to 7.9° (mean, 5.7°). The number of spikes fired over the course of the experiment ranged from 527 to 189,000 (mean, 17,900) and signal-to-noise ratios ranged from 1.2 to 12.6 (geometric mean, 3.0).

Figure 3 shows L and M cone weights across the cells we studied. Cone weights have been normalized such that the sum of their absolute values is equal to 1 (Johnson et al., 2004; Lennie, Krauskopf, & Sclar, 1990). Points close to the left and right edges of the bounding triangle therefore represent cells with low S cone weights, and points close to the origin represent cells with large S cone weights. Cone weights were heterogeneous across cells, but we could define two more-or-less discrete cell groups based on these cone weights. One group, shown as large black disks, had

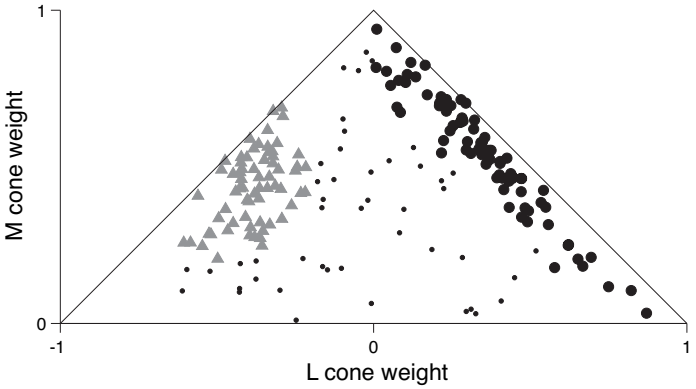

Figure 3. L and M cone weights for 190 V1 cells. Cone weights were normalized so the sum of their absolute values was equal to 1 (Johnson et al., 2004; Lennie et al., 1990). M cone weights were constrained to be positive. Cells with large positive L and M cone weights were defined as luminance cells (large black disks), cells with oppositely signed, similar magnitude L and M cone weights were defined as color cells (gray triangles), and cells with intermediate L and M cone weights were not included in either category (small black disks).

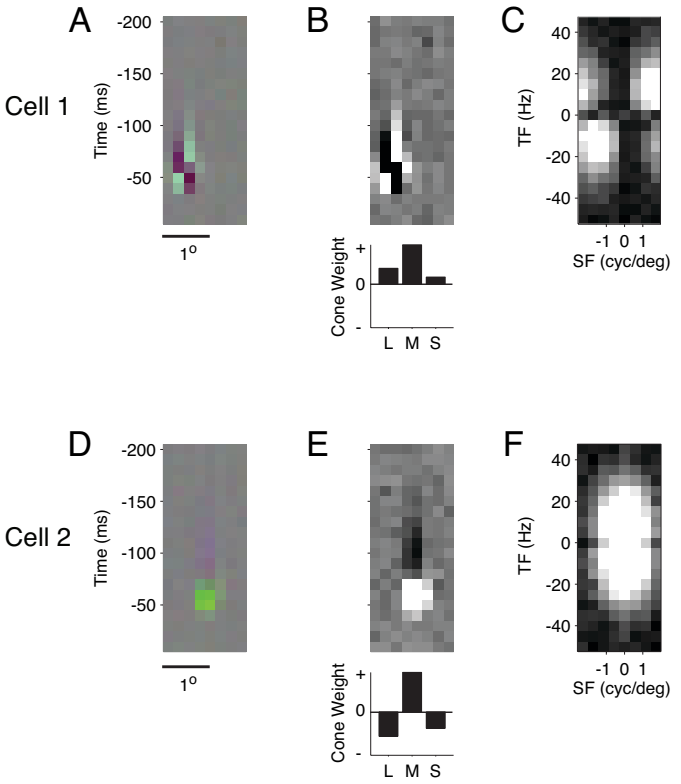

Figure 4. Space-time receptive fields for two neurons. A. A spatiotemporal slice through the spike-triggered average volume (Figure 2A) for a luminance-tuned cell. Each space-time pixel in this plot has a unique RGB triplet associated with it that represents the average color of the stimulus at that space-time pixel relative to spike occurrence. B. Spatiotemporal and chromatic weighting functions. The spike-triggered average was decomposed into a spatiotemporal weighting function (top) and a color weighting function, represented here as cone weights (bottom). C. Fourier power spectrum of the spatiotemporal weighting function. The power in each spatiotemporal frequency band is shown in grayscale. D, E, and F follow the same format as A, B, and C, respectively, but show data from a color-tuned cell.

identically signed L and M cone weights and thus will be referred to as the group of luminance-tuned cells. The other group, shown as gray triangles, had oppositely signed L and M cone weights of similar magnitude and will thus be referred to as the group of color cells. The precise criteria we used to classify cells were somewhat arbitrary, but, as we will show, the results we report are robust to the specifics of this division.

Space-time orientation analysis

Figure 4A shows an example space-time RF for a luminance neuron. Most of the pixels are roughly the same shade of gray as the background, which is expected of pixels that did not influence the firing probability. The lower left of the plot, however, contains a structured pattern of bright green and dark red pixels. The bright green and dark red represent opposite deviations from the background color and are roughly consistent with luminance ON and OFF signals, respectively, as shown below.

We separated the spatiotemporal weighting function (Figure 4B, top) from the cone weights (Figure 4B, bottom) by SVD. For this cell, all three cone weights were of identical sign, and the magnitudes of these weights were roughly consistent with luminance tuning. The spatiotemporal weighting function is obliquely oriented, consistent with direction selectivity.

To quantify the degree of oblique orientation in this spatiotemporal weighting function, we computed the 2D Fourier power spectrum, presented in Figure 4C. The DC component is at the center of the plot, and the power spectrum is constrained to be symmetric about this point. Most of the power is in the first and third quadrants, yielding an STOI of 0.52, which is one of the largest we observed.

The lower row of panels in Figure 4 shows data from a color-tuned neuron. The STA appears in Figure 4D, and in Figure 4E this average stimulus is separated into cone weights and a spatiotemporal weighting function. This neuron's RF was not space-time oriented, so its Fourier power was spread evenly over all four quadrants (Figure 4F). The STOI for this cell was 0.07.

Across the cells in our dataset, luminance-tuned cells had significantly higher STOIs than color-tuned cells did (median for luminance cells = 0.25 vs. median for color cells = 0.09, Mann-Whitney U-test: $p < .0001$). The histograms in Figure 5A and 5B show the distribution of STOIs for luminance and color cells, respectively. Some cells in

both categories had low STOIs, indicating poor space-time RF orientation. These cells cannot implement the filtering operation required by the first-order motion system. On the other hand, some cells had large STOIs, consistent with a role in the space-time filtering operation hypothesized to underlie the first-order motion system, and these neurons tended to be luminance tuned.

To confirm that this result was robust to the division of cells into color and luminance categories, we performed the analysis again treating all of the cells to the right of 0 in Figure 3 as luminance cells and all the cells to the left of 0 as color cells. This division between color and luminance cells did not change the result (median luminance STOI = 0.21 vs. median color STOI = 0.09, $p < .0001$). As an additional check, we dispensed with the luminance/color dichotomy and considered for each cell the sum of normalized L and M cone weights. This sum is largest for cells tuned close to luminance (L+M) and smallest for cells that are tuned for chromatic (L–M) modulation. The sum of normalized L and M cone weights was significantly correlated with the STOI (Spearman's r = 0.45, $p < .0001$), further reinforcing the idea that space-time RF orientation and luminance tuning tend to co-occur.

A systematic difference in the signal-to-noise ratio of color and luminance cells could lead artifactually to a systematic difference in their STOIs. We thus considered the joint distribution of STOIs and signal-to-noise ratios across our data set, shown in Figure 5B. Signal-to-noise ratios in the luminance- and color-tuned cell groups were not systematically different (median for luminance group: 2.7; median for color group: 3.0, Mann-Whitney U-test: $p = .26$). Moreover, the difference in STOIs between color and luminance cells was evident across the entire range of signal-to-noise ratios. For cells whose signal-to-noise ratio was smaller than the median value of 2.8, the difference in STOI was small but still significant (median STOI for luminance cells 0.20 vs. median STOI for color cells 0.09, $p < .01$). For cells for which we had cleaner data (signal-to-noise ratios above the median), the effect was more pronounced (0.35 for luminance vs. 0.09 for color, $p < .0001$).

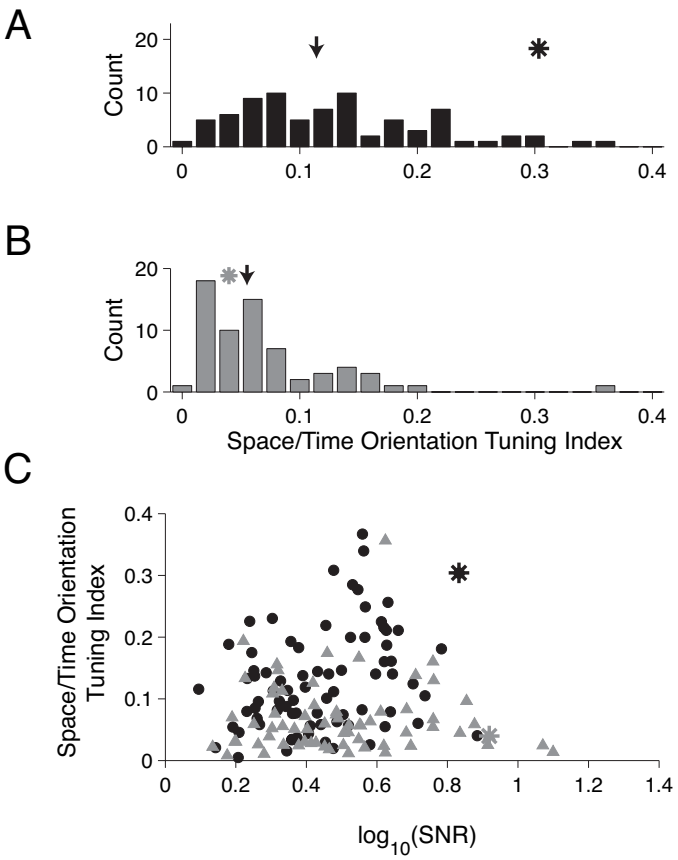

Figure 5. Distribution of the space-time orientation tuning index for 78 luminance cells (A) and 66 color cells (B). Arrows at the top of each histogram represent medians, and asterisks represent the example cells shown in Figure 4. Some luminance cells have strongly space-time oriented receptive fields (RFs), but few color cells do. C. Scatterplot relating the space-time orientation tuning index to the signal-to-noise ratio of the spike-triggered average. As expected, the value of the space-time orientation tuning index increases with the signal-to-noise ratio, but this does not account for the difference in the space-time RF orientation of luminance-tuned cells (black disks) and color-tuned cells (gray triangles).

Space-space orientation analysis

To determine whether the cells we classified into luminance and color categories differed with respect to their spatial orientation tuning, we computed for each cell a space-space orientation tuning index (SSOI). Figure 6A and 6B show spatial weighting functions and corresponding Fourier power spectra for the two example neurons shown in Figure 4. The RF of example neuron 1 (the luminance-tuned neuron) contained elongated ON and OFF subunits, whereas the RF of example neuron 2 (the color-tuned neuron) was roughly symmetrical and did not contain obvious subunits. This difference in RF structure leads to differences in power spectra and consequently to differences in SSOI.

Figure 6C shows the distribution of SSOI as a function of signal-to-noise ratio of the spatial weighting function. Across the population of neurons we studied, SSOIs were systematically greater for luminance cells than for color cells (median luminance SSOI = 0.92 vs. median color SSOI = 0.60, Mann-Whitney U-test: $p < .0001$). Similarly to our analysis of space-time orientation, this result was robust to our definitions of color and luminance cells (classifying cells on the basis of the sign of L+M weights: median luminance SSOI = 0.92 vs. median color SSOI = 0.66, $p < .0001$; correlating L+M and SSOI: Spearman's r = 0.30, $p < .0001$). Note, however, that the distributions of SSOIs for color and luminance cells were broad and overlapping,

indicating the presence of some strongly orientation-tuned color cells and poorly orientation-tuned luminance cells.

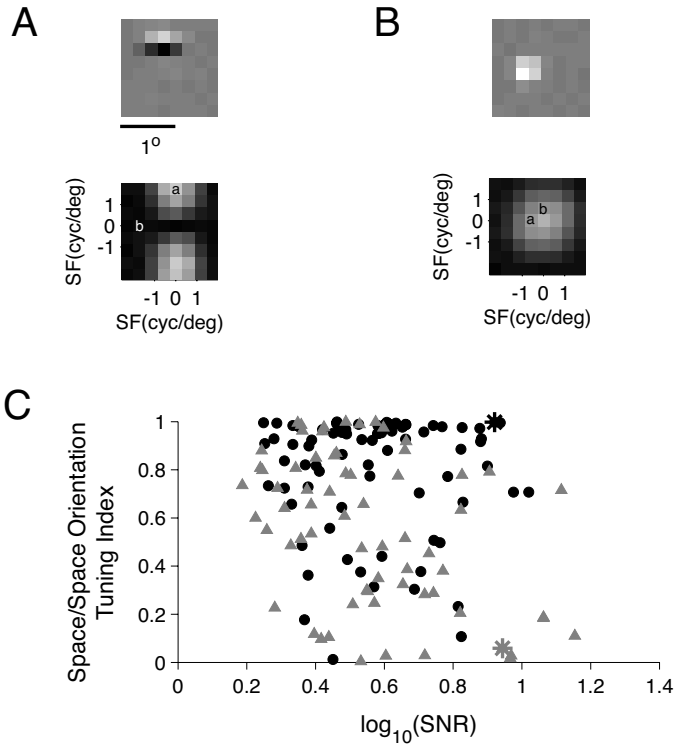

Figure 6. Analysis of spatial orientation tuning. A. Spatial weighting function for the example neuron in Figure 4A and corresponding power spectrum. The peak of the power spectrum is indicated by "a," and power at the orthogonal orientation (but the same spatial frequency) is indicated by "b." B. Data from the color-tuned neuron from Figure 4B. C. Space/space orientation tuning index as a function of signal-to-noise ratio for luminance cells (black disks) and color cells (gray triangles). Example neurons in A and B are represented by black and gray asterisks, respectively.

Discussion

The first-order motion system is particularly sensitive to luminance contrast, and its front end can be modeled as a bank of space-time oriented linear filters. The neural implementation of these filters may be V1 neurons with space-time oriented RFs. In this study we have strengthened this idea by demonstrating that such cells tend to be tuned preferentially for luminance.

Effects of stimulus statistics

Our stimulus largely modulated the three cone types together, so cone contrasts in cone isolating directions (e.g., changes L cone modulation conditional on M and S cone activation constrained to be at their mean levels) were modest: (L: 2.8%, M: 3.3%, and S: 22.3%). Nevertheless, responses of the neurons we classified into luminance (17.5 sp/s) and color (17.1 sp/s) categories were similar (Mann-Whitney U-test, $p = .7$) and yielded RF maps of similar quality (see Figure 5C). The lack of chromatic contrast in our stimulus is therefore unlikely to account for the lack of space-time oriented RFs among color-tuned cells.

The response latency of V1 cells is known to vary systematically with stimulus contrast (Albrecht, 1995). The color-tuned cells we studied had longer response latencies than the luminance-tuned cells under the conditions of our experiment, but this result may depend on the statistics of the stimulus we used. An important direction for future research is to explore the relationships among stimulus contrast, color tuning, and response dynamics.

Effects of chromatic aberration

We did not measure direction selectivity directly, but rather space-time RF orientation, which is a related but distinct response property. Our results are thus immune to an artifact that complicates direction-selectivity measurements made with conventional sharp-edged moving stimuli (e.g., moving bars). A sharp border between two equiluminant lights, once it is passed through the optics of the eye, contains a luminance artifact that moves along with the nominally equiluminant border. This artifact could elicit direction-selective responses in a luminance-tuned cell, thus giving the impression of sensitivity to chromatic motion (Faubert, Bilodeau, & Simonet, 2000). Low spatial frequency stimuli can mitigate this problem, but many direction-selective neurons have bandpass spatial tuning and therefore do not respond well to low spatial frequency stimuli.

Our stimulus contains sharp edges that, because of chromatic aberrations, were accompanied by chromoluminance artifacts. Importantly, however, these artifacts moved up, down, left, and right with equal probability and therefore would not be expected to manifest as spatiotemporal RF orientation. This is true irrespective of the color-tuning of the cell and the spectral content of the artifacts. We thus conclude that our central result, that neurons with space-time oriented RFs tend to be tuned for luminance, is not a trivial consequence of chromatic aberration. On the other hand, chromatic aberrations would bias our cone weight estimates if these artifacts were large relative to the color modulations in our display. This was not the case. Relative L and M cone activations in response to our stimulus varied by only ~5% between 0 and 8 cycles/deg as a result of axial chromatic aberration (Cottaris, 2003; Marimont & Wandell, 1994). Eighty-five percent of the power in our stimulus was within this range, suggesting that our estimates of relative L and M cone weight were affected little by chromatic aberration. A more detailed treatment of the impact of chromatic aberration on the retinal image of our stimulus can be found in Horwitz et al. (2005).

Color and motion in extrastriate cortex

Extrastriate area MT is specialized for processing visual motion and may be an important component of the first-order motion system. Most MT neurons are exquisitely sensitive to luminance contrast, but are not completely silenced at equiluminance (Dobkins & Albright, 1994; Gegenfurtner et al., 1994; Saito, Tanaka, Isono, Yasuda, & Mikami, 1989; Seidemann, Poirson, Wandell, & Newsome, 1999). These response properties are expected from the copious magnocellular input to MT neurons. Magnocellular neurons, while tuned closely for luminance, receive variable proportions of input from L and M cones, which results in a significant population response even at equiluminance (Lee, Martin, & Valberg, 1988; Logothetis, Schiller, Charles, & Hurlbert, 1990; Thiele, Dobkins, & Albright, 1999). Furthermore, magnocellular neurons do not combine cone inputs linearly and thus can respond to chromatic borders even though they are blind to the contrast sign across the border (Hubel & Livingstone, 1990; Kruger, 1979; Lee, Martin, & Valberg, 1989; Schiller & Colby, 1983; Shapley & Kaplan, 1989). Psychophysical studies have shown that when stimulus displacements are small (a manipulation intended to activate the first-order motion system selectively), chromatic motion is readily masked by luminance noise (Yoshizawa, Mullen, & Baker, 2000) and survives high temporal-frequency exchange of the colors that define the moving border (Dobkins & Albright, 1993). These phenomena may arise from the small chromatic component of magnocellular input to MT neurons.

On the other hand, some MT neurons respond remarkably well near equiluminance (Dobkins & Albright, 1994; Saito et al., 1989; Seidemann et al., 1999), suggesting that these neurons receive chromatic signals above and beyond those expected from magnocellular inputs alone (Thiele et al., 1999). Color-opponent V1 cells could contribute to the direction selectivity of MT neurons if their spatiotemporal pattern of connections were arranged so that sequential activation provided a greater input for one direction of motion than the opposite. This architecture is essentially identical to that believed to underlie the formation of space-time oriented RFs in V1: V1 simple cells are thought to acquire direction selectivity by integrating inputs from the lateral geniculate nucleus (LGN) with different spatial offsets and delays (De Valois, Cottaris, Mahon, Elfar, & Wilson, 2000; Livingstone, 1998). Similarly, an MT neuron could integrate inputs from color-opponent V1 neurons with spatially offset RFs and different lags. Of course, V1 RFs are larger than LGN RFs, so under this model, chromatic motion would require a greater stimulus displacement than luminant motion to result in a reliable neural signal. This model makes the testable prediction that MT neurons might exhibit greater sensitivity for lower spatial frequencies (larger spatial displacements) for chromatic motion relative to luminant motion.

Acknowledgments

We thank Bart Krekelberg and Lu Lesmes for helpful comments on the manuscript, and Dinh Diep, Doug Woods, and Jennifer Costanza for technical assistance. TDA is an investigator for the Howard Hughes Medical Institute.

Commercial relationships: none.
Corresponding author: Greg Horwitz.
Email: horwitz@salk.edu.
Address: The Salk Institute for Biological Studies, 10010 North Torrey Pines Road, La Jolla, CA 92037.

References

Adelson, E. H., & Bergen, J. R. (1985). Spatio-temporal energy models for the perception of motion. *Journal of the Optical Society of America A, 2*, 284-299. [PubMed]

Albrecht, D. G. (1995). Visual cortex neurons in monkey and cat: Effect of contrast on the spatial and temporal phase transfer functions. *Visual Neuroscience, 12*(6), 1191-1210. [PubMed]

Cavanagh, P., & Mather, G. (1989). Motion: The long and short of it. *Spatial Vision, 4*(2-3), 103-129. [PubMed]

Chichilnisky, E. J. (2001). A simple white noise analysis of neuronal light responses. *Network, 12*(2), 199-213. [PubMed]

Conway, B. R., Hubel, D. H., & Livingstone, M. S. (2002). Color contrast in macaque V1. *Cerebral Cortex, 12*(9), 915-925. [PubMed]

Conway, B. R., & Livingstone, M. S. (2003). Space-time maps and two-bar interactions of different classes of direction-selective cells in macaque V-1. *Journal of Neurophysiology, 89*(5), 2726-2742. [PubMed]

Cottaris, N. P. (2003). Artifacts in spatiochromatic stimuli due to variations in preretinal absorption and axial chromatic aberration: Implications for color physiology. *Journal of the Optical Society of America A, 20*(9), 1694-1713. [PubMed]

De Valois, R. L., Cottaris, N. P., Mahon, L. E., Elfar, S. D., & Wilson, J. A. (2000). Spatial and temporal receptive fields of geniculate and cortical cells and directional selectivity. *Vision Research, 40*(27), 3685-3702. [PubMed]

Dobkins, K. R., & Albright, T. D. (1993). What happens if it changes color when it moves? Psychophysical experiments on the nature of chromatic input to motion detectors. *Vision Research, 33*(8), 1019-1036. [PubMed]

Dobkins, K. R., & Albright, T. D. (1994). What happens if it changes color when it moves? The nature of chromatic input to macaque visual area MT. *Journal of Neuroscience, 14*(8), 4854-4870. [PubMed]

Emerson, R. C. (1997). Quadrature subunits in directionally selective simple cells: Spatiotemporal interactions. *Visual Neuroscience, 14*(2), 357-371. [PubMed]

Faubert, J., Bilodeau, L., & Simonet, P. (2000). Transverse chromatic aberration and colour-defined motion. *Opthalmic and Physiological Optics, 20*(4), 274-280. [PubMed]

Gegenfurtner, K. R., Kiper, D. C., Beusmans, J. M., Carandini, M., Zaidi, Q., & Movshon, J. A. (1994). Chromatic properties of neurons in macaque MT. *Visual Neuroscience, 11*(3), 455-466. [PubMed]

Gouras, P. (1974). Opponent-color cells in different layers of foveal striate cortex. *Journal of Physiology, 238*, 583-602. [PubMed]

Horwitz, G. D., Chichilnisky, E. J., & Albright, T. D. (2005). Blue-yellow signals are enhanced by spatiotemporal luminance contrast in macaque V1. *Journal of Neurophysiology, 93*(4), 2263-2278. [PubMed]

Hubel, D. H., & Livingstone, M. S. (1990). Color and contrast sensitivity in the lateral geniculate body and primary visual cortex of the macaque monkey. *Journal of Neuroscience, 10*(7), 2223-2237. [PubMed]

Johnson, E. N., Hawken, M. J., & Shapley, R. (2004). Cone inputs in macaque primary visual cortex. *Journal of Neurophysiology, 91*(6), 2501-2514. [PubMed]

Knoblauch, K., & D'Zmura, M. (2001). Reply to letter to editor by M.J. Sankeralli and K.T. Mullen, *Vision Research*, *41*, 53-55: Lights and neural responses do not depend on choice of color space. *Vision Research, 41*(13), 1683-1684. [PubMed]

Kruger, J. K. (1979). Responses to wavelength contrast in the afferent visual systems of the cat and the rhesus monkey. *Vision Research, 19*(12), 1351-1358. [PubMed]

Lee, B. B., Martin, P. R., & Valberg, A. (1988). The physiological basis of heterochromatic flicker photometry demonstrated in the ganglion cells of the macaque retina. *Journal of Physiology, 404*, 323-347. [PubMed]

Lee, B. B., Martin, P. R., & Valberg, A. (1989). Nonlinear summation of M- and L-cone inputs to phasic retinal ganglion cells of the macaque. *Journal of Neuroscience, 9*(4), 1433-1442. [PubMed]

Lennie, P., Krauskopf, J., & Sclar, G. (1990). Chromatic mechanisms in striate cortex of macaque. *Journal of Neuroscience., 10*, 649-669. [PubMed]

Leventhal, A. G., Thompson, K. G., Liu, D., Zhou, Y., & Ault, S. J. (1995). Concomitant sensitivity to orientation, direction, and color of cells in layers 2, 3, and 4 of monkey striate cortex. *Journal of Neuroscience, 15*(3 Pt 1), 1808-1818. [PubMed]

Livingstone, M. S. (1998). Mechanisms of direction selectivity in macaque V1. *Neuron, 20*(3), 509-526. [PubMed]

Livingstone, M. S., & Conway, B. R. (2003). Substructure of direction-selective receptive fields in macaque V1. *Journal of Neurophysiology, 89*(5), 2743-2759. [PubMed]

Livingstone, M. S., & Hubel, D. H. (1984). Anatomy and physiology of a color system in the primate visual cortex. *Journal of Neuroscience, 4*, 309-356. [PubMed]

Logothetis, N. K., Schiller, P. H., Charles, E. R., & Hurlbert, A. C. (1990). Perceptual deficits and the activity of the color-opponent and broad-band pathways at isoluminance. *Science, 247*, 214-217. [PubMed]

Marimont, D. H., & Wandell, B. A. (1994). Matching color images: The impact of axial chromatic aberration. *Journal of the Optical Society of America A, 111*, 3113-3122.

McLean, J., & Palmer, L. A. (1989). Contribution of linear spatiotemporal receptive field structure to velocity selectivity of simple cells in area 17 of cat. *Vision Research, 29*, 675-679. [PubMed]

Michael, C. R. (1978a). Color vision mechanisms in monkey striate cortex: Simple cells with dual opponent-color receptive fields. *Journal of Neurophysiology, 41*(5), 1233-1249. [PubMed]

Michael, C. R. (1978b). Color-sensitive complex cells in monkey striate cortex. *Journal of Neurophysiology, 41*(5), 1250-1266. [PubMed]

Reid, R. C., Soodak, R. E., & Shapley, R. M. (1987). Linear mechanisms of directional selectivity in simple cells of cat striate cortex. *Proceedings of the National Academy of Arts and Sciences U.S.A., 84*, 8740-8744. [PubMed][Article]

Saito, H., Tanaka, K., Isono, H., Yasuda, M., & Mikami, A. (1989). Directionally selective response of cells in the middle temporal area (MT) of the macaque monkey to the movement of equiluminous opponent color stimuli. *Experimental Brain Research, 75*(1), 1-14. [PubMed]

Schiller, P. H., & Colby, C. L. (1983). The responses of single cells in the lateral geniculate nucleus of the rhesus monkey to color and luminance contrast. *Vision Research, 23*(12), 1631-1641. [PubMed]

Seidemann, E., Poirson, A. B., Wandell, B. A., & Newsome, W. T. (1999). Color signals in area MT of the macaque monkey. *Neuron, 24*(4), 911-917. [PubMed]

Shapley, R., & Kaplan, E. (1989). Responses of magnocellular LGN neurons and M retinal ganglion cells to drifting heterochromatic gratings. *Investigative Ophthalmology and Visual Science* (Suppl.), *30*, 323.

Stockman, A., MacLeod, D. I., & Johnson, N. E. (1993). Spectral sensitivities of the human cones. *Journal of the Optical Society of America A, 10*(12), 2491-2521. [PubMed]

Strang, G. (1988). *Linear algebra and its applications* (3rd ed.). San Diego: Harcourt, Brace, Jovanovich.

Tamura, H., Sato, H., Katsuyama, N., Hata, Y., & Tsumoto, T. (1996). Less segregated processing of visual information in V2 than in V1 of the monkey visual cortex. *European Journal of Neuroscience, 8*(2), 300-309. [PubMed]

Thiele, A., Dobkins, K. R., & Albright, T. D. (1999). The contribution of color to motion processing in Macaque middle temporal area. *Journal of Neuroscience, 19*(15), 6571-6587. [PubMed]

Watson, A. B., & Ahumada, A. J. (1985). Model of human visual-motion sensing. *Journal of the Optical Society of America A, 2*, 322-341. [PubMed]

Yoshizawa, T., Mullen, K. T., & Baker, C. L., Jr. (2000). Absence of a chromatic linear motion mechanism in human vision. *Vision Research, 40*(15), 1993-2010. [PubMed]